

Communication: State-to-state photoionization and photoelectron study of vanadium methylidyne radical (VCH)

Zhihong Luo, Zheng Zhang, Huang Huang, Yih-Chung Chang, and C. Y. Ng

Citation: *The Journal of Chemical Physics* **140**, 181101 (2014); doi: 10.1063/1.4876017

View online: <http://dx.doi.org/10.1063/1.4876017>

View Table of Contents: <http://scitation.aip.org/content/aip/journal/jcp/140/18?ver=pdfcov>

Published by the [AIP Publishing](#)

Articles you may be interested in

[Rovibronically selected and resolved two-color laser photoionization and photoelectron study of titanium monoxide cation](#)

J. Chem. Phys. **138**, 174309 (2013); 10.1063/1.4803161

[Photoelectron spectroscopic study of the Ee Jahn–Teller effect in the presence of a tunable spin–orbit interaction. I. Photoionization dynamics of methyl iodide and rotational fine structure of CH₃I⁺ and CD₃I⁺](#)

J. Chem. Phys. **134**, 054308 (2011); 10.1063/1.3547548

[Rovibrationally selected and resolved state-to-state photoionization of ethylene using the infrared-vacuum ultraviolet pulsed field ionization-photoelectron method](#)

J. Chem. Phys. **125**, 133304 (2006); 10.1063/1.2213261

[Photoelectron spectroscopy and density functional theory of puckered ring structures of Group 13 metal-ethylenediamine](#)

J. Chem. Phys. **121**, 7692 (2004); 10.1063/1.1791633

[Ionization from a double bond: Rovibronic photoionization dynamics of ethylene, large amplitude torsional motion and vibronic coupling in the ground state of C₂H₄⁺](#)

J. Chem. Phys. **120**, 1761 (2004); 10.1063/1.1635815



computing
SCIENCE & ENGINEERING

AIP'S JOURNAL OF COMPUTATIONAL TOOLS AND METHODS.
AVAILABLE AT MOST LIBRARIES.

Communication: State-to-state photoionization and photoelectron study of vanadium methyldyne radical (VCH)

Zhihong Luo, Zheng Zhang, Huang Huang, Yih-Chung Chang, and C. Y. Ng^{a)}

Department of Chemistry, University of California, Davis, California 95616, USA

(Received 6 April 2014; accepted 30 April 2014; published online 12 May 2014)

By employing the infrared (IR)-ultraviolet (UV) laser excitation scheme, we have obtained rotationally selected and resolved pulsed field ionization-photoelectron (PFI-PE) spectra for vanadium methyldyne cation (VCH⁺). This study supports that the ground state electronic configuration for VCH⁺ is $\dots 7\sigma^2 8\sigma^2 3\pi^4 9\sigma^1$ ($\tilde{X}^2\Sigma^+$), and is different from that of $\dots 7\sigma^2 8\sigma^2 3\pi^4 1\delta^1$ ($\tilde{X}^2\Delta$) for the isoelectronic TiO⁺ and VN⁺ ions. This observation suggests that the addition of an H atom to vanadium carbide (VC) to form VCH has the effect of stabilizing the 9σ orbital relative to the 1δ orbital. The analysis of the state-to-state IR-UV-PFI-PE spectra has provided precise values for the ionization energy of VCH, $IE(\text{VCH}) = 54\,641.9 \pm 0.8 \text{ cm}^{-1}$ ($6.7747 \pm 0.0001 \text{ eV}$), the rotational constant $B^+ = 0.462 \pm 0.002 \text{ cm}^{-1}$, and the v_2^+ bending ($626 \pm 1 \text{ cm}^{-1}$) and v_3^+ V-CH stretching ($852 \pm 1 \text{ cm}^{-1}$) vibrational frequencies for VCH⁺($\tilde{X}^2\Sigma^+$). The $IE(\text{VCH})$ determined here, along with the known $IE(\text{V})$ and $IE(\text{VC})$, allows a direct measure of the change in dissociation energy for the V-CH as well as the VC-H bond upon removal of the 1δ electron of VCH($\tilde{X}^3\Delta_1$). The formation of VCH⁺($\tilde{X}^2\Sigma^+$) from VCH($\tilde{X}^3\Delta_1$) by photoionization is shown to strengthen the VC-H bond by 0.3559 eV, while the strength of the V-CH bond remains nearly unchanged. This measured change of bond dissociation energies reveals that the highest occupied 1δ orbital is nonbonding for the V-CH bond; but has anti-bonding or destabilizing character for the VC-H bond of VCH($\tilde{X}^3\Delta_1$).

© 2014 AIP Publishing LLC. [<http://dx.doi.org/10.1063/1.4876017>]

Accurate structural and energetic measurements of transition metal carbides (MC) and methyldynes (MCH) and their cations (MC⁺ and MCH⁺) are essential for fundamental understanding of catalytic processes, such as the chemical activation of C-H and C-C bonds in hydrocarbon reactions, involving transition metal species as the catalyst.¹ Previous rotationally resolved spectroscopic studies have provided precise spectroscopic constants and thus structural parameters for many neutral MC and MCH species.²⁻⁸ However, similar rotationally resolved spectroscopic studies on MC⁺ and MCH⁺ ions are lacking. We have recently succeeded in performing high-resolution pulsed field ionization-photoelectron (PFI-PE)^{9,10} studies for diatomic MX⁺ (X = C, O, and N) species based on two-color visible-ultraviolet (VIS-UV) excitation scheme, which has allowed fully rotationally selected and resolved spectroscopic measurement for MX⁺ cations.¹¹⁻¹⁶ These studies have not only provided reliable rovibrational constants, but also accurate ionization energies (IEs) of MXs. To our knowledge, a fully rotationally resolved PFI-PE measurement for triatomic transition metal-containing cations has not been reported previously. This communication presents such a high-resolution photoelectron study for vanadium methyldyne cation (VCH⁺) using the infrared (IR)-UV-PFI-PE method.

The previous high-resolution spectroscopic study^{3,4} has established that the VCH ground state is linear with the electronic configuration of $\dots 7\sigma^2 8\sigma^2 3\pi^4 9\sigma^1 1\delta^1$ ($\tilde{X}^3\Delta_1$). Highly

precise values for the rotational constant B'' (0.49369 cm^{-1}) and the v_2 bending (564 cm^{-1}) and v_3 V-CH stretching (838 cm^{-1}) vibrational frequencies of VCH($\tilde{X}^3\Delta_1$) have also been determined.³ The highly precise $IE(\text{VCH})$ determined here, together with the known $IE(\text{V})$ ¹⁷ and $IE(\text{VC})$,¹⁶ is most valuable for benchmarking theoretical energetic predictions^{10,18} for the VCH/VCH⁺ system because the 0 K bond dissociation energies (D_0 's) for the V⁺-CH and V-CH bonds are related to the $IE(\text{V})$ and $IE(\text{VCH})$ by the relation, $D_0(\text{V}^+-\text{CH}) - D_0(\text{V}-\text{CH}) = IE(\text{V}) - IE(\text{VCH})$ based on conservation of energy.¹⁸ Similarly, the D_0 values for the VC⁺-H and VC-H bonds are related to the $IE(\text{VC})$ and $IE(\text{VCH})$ as $D_0(\text{VC}^+-\text{H}) - D_0(\text{VC}-\text{H}) = IE(\text{VC}) - IE(\text{VCH})$. We note that a value of $4.94 \pm 0.09 \text{ eV}$ for $D_0(\text{V}^+-\text{CH})$ was obtained in a previous collision-induced ion dissociation study.¹⁹

The experimental apparatus and procedures used are similar to those reported previously.¹²⁻¹⁵ Cold VCH molecules in the form of a pulsed supersonic beam (30 Hz) were prepared by using a laser ablation beam source.²⁰ The VCH molecules were produced in the ablation source by reactions between laser ablated V species and CH₄. The VCH supersonic beam passes through a conical skimmer before intersecting the laser beams at the photoionization/photoexcitation (PI/PEX) center for photoionization efficiency (PIE) and PFI-PE measurements. Two tunable dye lasers pumped by the same Nd:YAG laser (30 Hz) were used. One dye laser provided the IR ω_1 output and the other gave the UV ω_2 output as required by the experiment. A dc electric field was used to extract photoions from the PI/PEX region for PIE measurements. The PFI-PE

^{a)}Email: cyng@ucdavis.edu

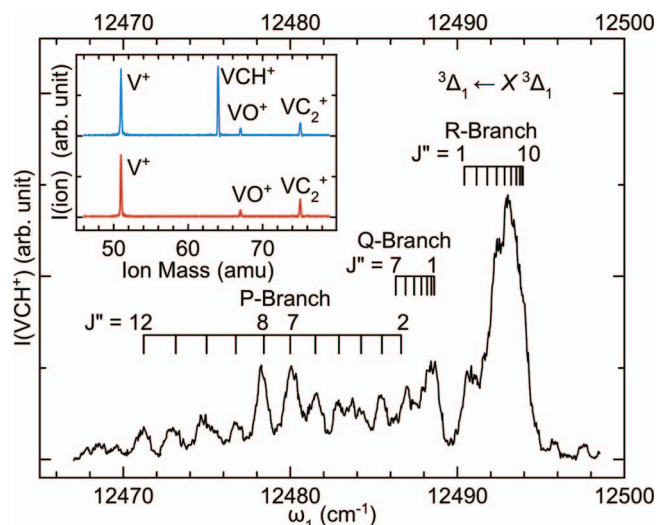


FIG. 1. The $VCH^*(^3\Delta_1) \leftarrow (\bar{X}^3\Delta_1; 000)$ excitation band recorded by setting $\omega_2 = 43\,022.76\text{ cm}^{-1}$ and scanning ω_1 in the range of $12\,467\text{--}12\,499\text{ cm}^{-1}$. Rotational transitions of the P, Q, R-branch identified by simulation are marked on top of the spectrum. The inset compares the TOF mass spectrum for the molecular beam observed by setting $\omega_1 = 12\,493$ and $\omega_2 = 42\,274\text{ cm}^{-1}$ with that (lower curve) recorded under the same experimental conditions except with the ω_1 beam off. The comparison shows that VCH^+ ions are only formed by IR-UV photoionization.

measurements were made by employing a pulsed PFI-PE detection scheme as described in detail previously.^{12–15}

The well-characterized $VCH^*(^3\Delta_1)$ band³ at 800.5 nm is selected to prepare the intermediate state for IR-UV-PIE and IR-UV-PFI-PE studies. By fixing UV $\omega_2 = 43\,022.76\text{ cm}^{-1}$ and scanning IR ω_1 in the range of $12\,467\text{--}12\,499\text{ cm}^{-1}$, the detection of VCH^+ ions thus produced yields the excitation spectrum for the $VCH^*(^3\Delta_1)$ band as shown in Fig. 1. Although the resolution of this spectrum was significantly lower than that achieved in the previous higher resolution study³ of Barnes *et al.*, we are still able to identify several well-resolved rotational transitions. The assigned rotational transitions for the P, Q, and R branches as marked on top of the excitation spectrum were based on spectral simulation using the spectroscopic constants reported³ previously. The relatively strong P(7) and P(8) rotational transitions were used for the respective single $J' = 6$ and $J' = 7$ selected IR-UV-PFI-PE measurements. The most intense peak of the excitation spectrum is the R-branch band head at $12\,493\text{ cm}^{-1}$. Selecting this peak by IR ω_1 gives the highest PIE and PFI-PE signals for IR-UV measurements. However, due to spectral congestion, the simulation shows that IR excitation at the R-branch band head would result in simultaneous excitations of the $J' = 5, 6, 7, 8,$ and 9 levels of $VCH^*(^3\Delta_1)$.

The inset of Fig. 1 compares the TOF mass spectrum (upper spectrum) of the molecular beam recorded by setting $\omega_1 = 12\,493\text{ cm}^{-1}$ and $\omega_2 = 42\,274\text{ cm}^{-1}$ and that (lower spectrum) obtained under the same experimental conditions except that the ω_1 beam was blocked. The VCH^+ peak is found to be discernible only as both ω_1 and ω_2 beams are turned on, confirming that VCH^+ ions are produced solely by IR-UV photoionization of VCH. The fact that the V^+ , VO^+ , and VC_2^+ ion intensities are nearly identical with or without the ω_1 beam indicates that these ions are produced by two-photon

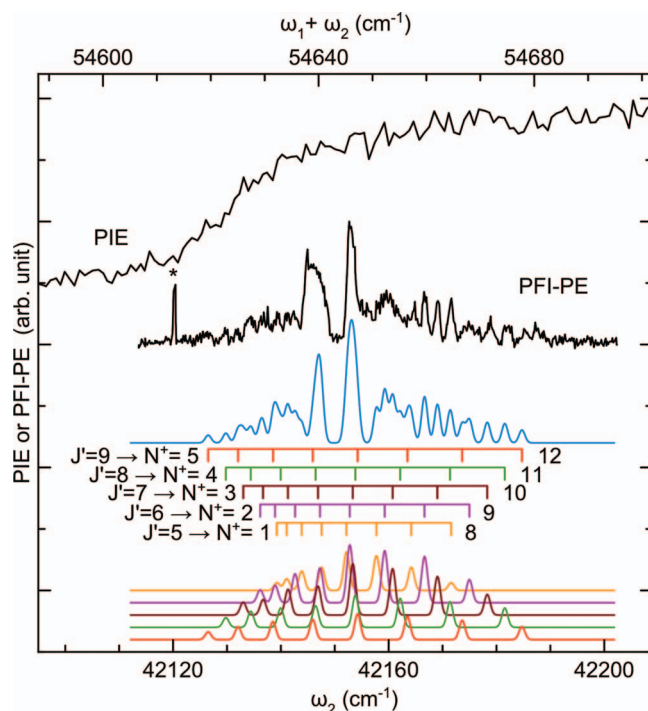


FIG. 2. Comparison of the IR-UV-PIE spectrum (top curve) and the IR-UV-PFI-PE spectrum (2nd curve from the top) for the $VCH^+(\bar{X}^2\Sigma^+; 000)$ origin band recorded by setting $\omega_1 = 12\,493\text{ cm}^{-1}$ and scanning the ω_2 in the range of $42\,095\text{--}42\,209\text{ cm}^{-1}$. The best simulated spectrum (blue curve) for the IR-UV-PFI-PE origin band represents the sum of the simulated $J' (= 5, 6, 7, 8,$ and $9) \rightarrow N^+$ state-to-state spectra (bottom curves) shown as the orange, purple, brown, green, and red spectra, respectively.

and/or multiphoton UV photoionization of impurity species in the molecular beam.

By parking ω_1 at $12\,493\text{ cm}^{-1}$ and scanning ω_2 in the energy range of $42\,095\text{--}42\,209\text{ cm}^{-1}$, which corresponds to the total energy ($\omega_1 + \omega_2$) range of $54\,588\text{--}54\,702\text{ cm}^{-1}$, we obtained the IR-UV-PIE spectrum for VCH^+ shown as the top spectrum of Fig. 2. The PIE spectrum exhibits a step-like structure at the total energy range of $54\,610\text{--}54\,640\text{ cm}^{-1}$. After taking into account the Stark shift induced by the dc electric field used for ion extraction, we obtained the $IE(VCH) = 54\,640 \pm 14\text{ cm}^{-1}$.

The location of the PIE step allows the PFI-PE measurement for the $VCH^+(\bar{X}; v_1^+v_2^+v_3^+ = 000)$ origin band to be focused in a narrower energy range. Figures 3(a) and 3(b) depict the $J' = 6$ and $J' = 7$ selected IR-UV-PFI-PE spectra (black curves) for the origin band obtained by setting ω_1 to excite the P(7) and P(8) transitions at $12\,480.05\text{ cm}^{-1}$ and $12\,478.26\text{ cm}^{-1}$, respectively, while scanning ω_2 in the range of $42\,121\text{--}42\,183\text{ cm}^{-1}$. The sharp structures marked by asterisks in the figures are attributed to background resonances originated from photoionization of V atoms, which are produced in abundance by the laser ablation source. Excluding these background peaks reveals a series of well-resolved rotational transitions with intensity patterns similar to those observed in previous two-color state-to-state PFI-PE measurements of other molecular systems.^{12–15,21,22} The blue spectra of Figs. 3(a) and 3(b) are the best simulated spectra constructed by assuming a Gaussian instrumental profile (FWHM = 1.3 cm^{-1}) for the PFI-PE detection. The

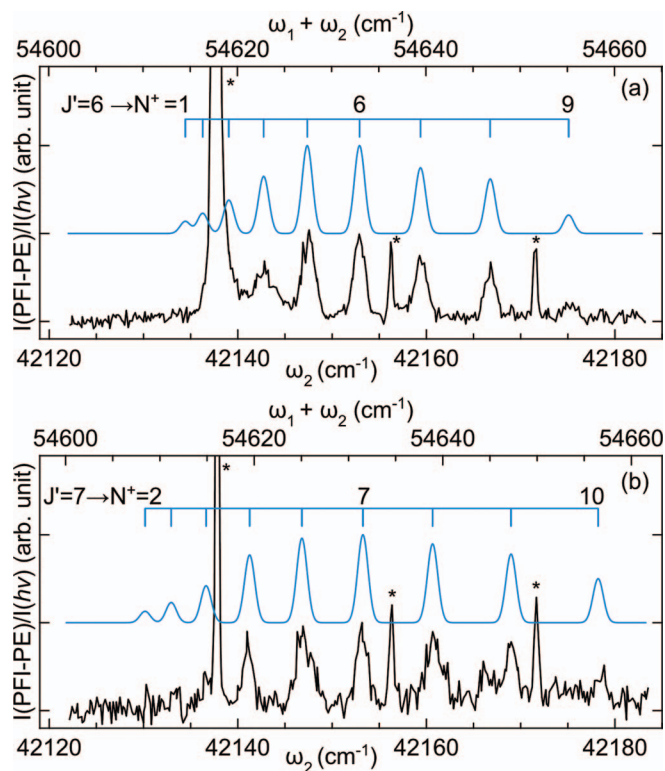


FIG. 3. (a) The $J' = 6$ and (b) $J' = 7$ selected IR-UV-PFI-PE spectra for the $\text{VCH}^+(\tilde{X}^2\Sigma^+; 000)$ origin band obtained by setting the $\omega_1 = 12\,480.05$ and $12\,478.26\text{ cm}^{-1}$, respectively. The blue curves are the simulated state-to-state spectra constructed by using a Gaussian instrumental profile (FWHM = 1.3 cm^{-1}) for the PFI-PE detection. The N^+ -assignments are marked on top of the simulated spectra.

N^+ -assignments marked in Figs. 3(a) and 3(b) are based on the least square fits to the standard equation, $\nu^+ = \nu_{000}^+ + B^+N^+(N^++1) - B''J''(J''+1)$, where ν^+ represents the photoionization transition frequency, ν_{000}^+ is the transition frequency for the origin of the origin band, and B'' and B^+ are the respective rotational constants for the $\text{VCH}(\tilde{X}; 000)$ and $\text{VCH}^+(\tilde{X}; 000)$ ground states. Since the rotational constant B'' for $\text{VCH}(\tilde{X}^3\Delta_1)$ is known, the least square fits for the IR-UV-PFI-PE spectra provide the values, $B^+ = 0.462 \pm 0.002\text{ cm}^{-1}$ and $\nu_{000}^+ = 54\,642.9 \pm 0.8\text{ cm}^{-1}$ after correcting for the Stark shift¹³ induced by the PFI electric field. The latter value gives the adiabatic $\text{IE}(\text{VCH}) = 54\,641.9 \pm 0.8\text{ cm}^{-1}$ ($6.7747 \pm 0.0001\text{ eV}$).

As shown in the rotational assignment of the IR-UV-PFI-PE spectrum of Fig. 3(a), the $J' = 6 \rightarrow N^+ = 4-9$ rotational peaks are clearly discernible. The formation of the $N^+ = 2$ and 3 rotational peaks was obscured by the strong background peak at $\omega_2 = 42\,137.8\text{ cm}^{-1}$. A minute structure appears to coincide with the simulated positions of the $N^+ = 1$ rotational peaks. However, since this structure is close to the noise level, its identification must be considered as tentative. The simulation of the IR-UV-PFI-PE spectra of Fig. 3(b) clearly identifies the $N^+ = 2-10$ rotational peaks. The intensity patterns for the $J' \rightarrow N^+$ transitions observed in Figs. 3(a) and 3(b) are consistent with those found in previous two-color state-to-state photoionization studies,^{12-15,21,22} showing that the $|\Delta N^+| = |N^+ - J'|$ changes are ≤ 5 , and the photoionization cross section increases as $|\Delta N^+|$ decreases.

Vanadium methylidyne is isoelectronic with vanadium nitride (VN)¹⁵ and titanium monoxide (TiO),¹⁴ and these species are known to have the same ground state electronic configuration^{6,7} of $\dots 7\sigma^2 8\sigma^2 3\pi^4 1\delta^1 9\sigma^1$ ($\tilde{X}^3\Delta_1$). The recent VIS-UV-PFI-PE studies^{14,15} show that photoionization of VN and TiO gives the $\text{VN}^+(\tilde{X}^2\Delta_{3/2})$ and $\text{TiO}^+(\tilde{X}^2\Delta_{3/2})$ ground states with the electronic configuration of $\dots 7\sigma^2 8\sigma^2 3\pi^4 1\delta^1$. The determination of the $\text{VN}^+(\tilde{X}^2\Delta_{3/2})$ and $\text{TiO}^+(\tilde{X}^2\Delta_{3/2})$ ground states is further confirmed by the observation of the excited $\text{VN}^+(\tilde{X}^2\Delta_{5/2})$ and $\text{TiO}^+(\tilde{X}^2\Delta_{5/2})$ spin-orbit states at 307.3 and 211.3 cm^{-1} above the $\text{VN}^+(\tilde{X}^2\Delta_{3/2})$ and $\text{TiO}^+(\tilde{X}^2\Delta_{3/2})$ ground states, respectively.^{14,15} Since the IR-UV-PFI-PE spectra of Figs. 3(a) and 3(b) cannot identify the lowest N^+ value, the term symmetry of the $\text{VCH}^+(\tilde{X})$ ground state cannot be directly determined. However, if the $\text{VCH}^+(\tilde{X})$ ion ground state were of $^2\Delta_{3/2}$ symmetry, we should have observed the excited $^2\Delta_{5/2}$ spin-orbit state for VCH^+ at $\approx 200-300\text{ cm}^{-1}$ above the $\text{VCH}^+(\tilde{X})$ ground state. Considering the fact that such an excited spin-orbit state was not found in a careful search, we conclude that the $\text{VCH}^+(\tilde{X})$ ground state is of $^2\Sigma^+$ symmetry with the electronic configuration of $\dots 7\sigma^2 8\sigma^2 3\pi^4 9\sigma^1$. That is, photoionization of $\text{VCH}(\tilde{X}^3\Delta_1)$ to form $\text{VCH}^+(\tilde{X}^2\Sigma^+)$ involves the removal of the electron residing in the 1δ instead of the 9σ orbital as in the case of TiO and VN .^{6,7,14,15} This observation suggests that the addition of an H atom to VC to form $\text{VCH}(\tilde{X}^3\Delta_1)$ has the effect of stabilizing the 9σ orbital, such that photoionization of VCH favors the ejection of an electron from the 1δ orbital. Titanium methylidyne (TiCH)⁵ is isoelectronic with VCH^+ . The fact that the $\text{TiCH}(\tilde{X})$ ground state is found to have the $^2\Sigma^+$ symmetry⁵ can be taken as strong support for the symmetry assignment of $\text{VCH}^+(\tilde{X}^2\Sigma^+)$ in the present study.

Using the known $\text{IE}(\text{V}) = 6.7463 \pm 0.0001\text{ eV}$ ¹⁷ and the $\text{IE}(\text{VCH}) = 6.7747 \pm 0.0001\text{ eV}$ determined in the present study, the difference $D_0(\text{V}^+-\text{CH}) - D_0(\text{V}-\text{CH})$ is determined to be -0.0284 eV . The $\text{IE}(\text{VC})$ has recently been determined to be $7.1306 \pm 0.0001\text{ eV}$.¹⁶ By combining this value with the $\text{IE}(\text{VCH})$, we find that the $D_0(\text{VC}^+-\text{H})$ is stronger than the $D_0(\text{VC}-\text{H})$ by $0.3559 \pm 0.0001\text{ eV}$. This observed D_0 change reveals the highest occupied 1δ orbital is nonbonding in nature for the $\text{V}-\text{CH}$ bond; but has anti-bonding or destabilizing character for the $\text{VC}-\text{H}$ bond of $\text{VCH}(\tilde{X}^3\Delta_1)$.

The PFI-PE signal was too low for single J' -selected IR-UV-PFI-PE measurements of the excited $\text{VCH}^+(\tilde{X}^2\Sigma^+; \nu_1^+\nu_2^+\nu_3^+ = 010$ and $001)$ vibrational bands. These bands are expected to appear at ≈ 600 and 850 cm^{-1} above the $\text{IE}(\text{VCH})$ based on the known ν_2 bending and ν_3 $\text{V}-\text{CH}$ stretching vibrational frequencies of $\text{VCH}(\tilde{X}^3\Delta_1)$.³ By parking the IR ω_1 at the R-branch band head of the $\text{VCH}^*(\tilde{X}^3\Delta_1)$ band, we have obtained the IR-UV-PFI-PE spectra for the excited $\text{VCH}^+(\tilde{X}^2\Sigma^+; 010$ and $001)$ vibrational bands [top spectra of Figs. 4(a) and 4(b)]. We have also measured the IR-UV-PFI-PE spectrum (black spectrum of Fig. 2) for the $\text{VCH}^+(\tilde{X}^2\Sigma^+; 000)$ origin band under the same experimental conditions for comparison with the single J' -selected IR-UV-PFI-PE of Figs. 3(a) and 3(b). Such a comparison is useful for validating the simulation scheme employed in this study.

The best simulated spectra for the (000), (010), and (001) IR-UV-PFI-PE bands [shown as the blue spectra in

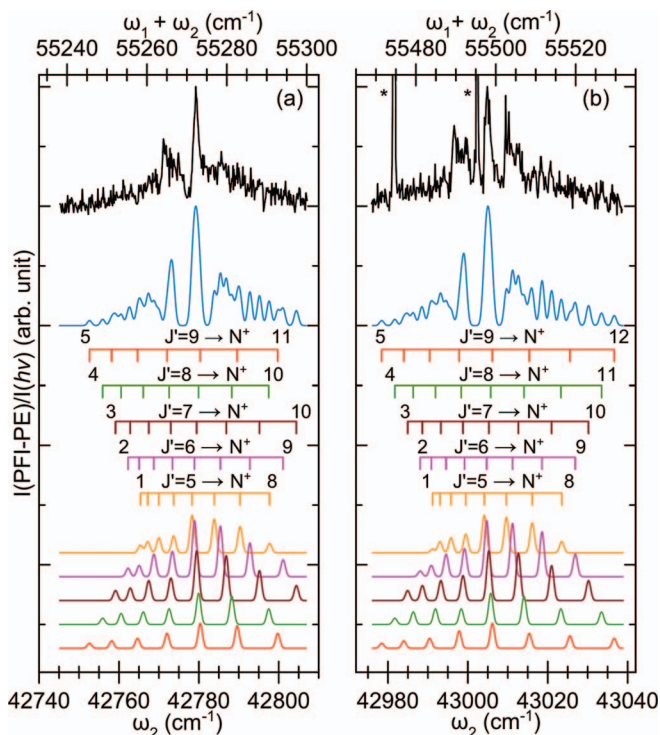


FIG. 4. Comparison of the IR-UV-PFI-PE spectra (top spectra) and the best simulated spectra (blue spectra) for the (a) $\text{VCH}^+(\tilde{X}^2\Sigma^+; 010)$ and (b) $\text{VCH}^+(\tilde{X}^2\Sigma^+; 001)$ vibrational bands. The IR-UV-PFI-PE spectra are obtained by setting the $\omega_1 = 12\,493\text{ cm}^{-1}$ and scanning ω_2 in the $42\,745\text{--}42\,807\text{ cm}^{-1}$ for (a) and $42\,975\text{--}43\,038\text{ cm}^{-1}$ for (b). The best simulated spectra represent the sum of the simulated J' ($= 5, 6, 7, 8,$ and 9) $\rightarrow N^+$ state-to-state spectra (bottom spectra) shown as the orange, purple, brown, green, and red spectra, respectively.

Figs. 2, 4(a), and 4(b)] are obtained by summing the simulated J' ($= 5, 6, 7, 8,$ and 9) $\rightarrow N^+$ spectra (bottom spectra), which are shown as the orange, purple, brown, green, and red spectra, respectively. The simulation^{12–15} assumes a Gaussian instrumental profile (FWHM = 1.3 cm^{-1}) for the PFI-PE detection and takes into account the bandwidth of ω_1 , the Boltzmann populations of J' -rotational levels based on an estimated rotational temperature of 35 K for the VCH molecular beam, and the overlaps of the rotational transitions with the excitation profile of the ω_1 output. The ΔN^+ -dependence of the photoionization cross sections follows the patterns observed in the present and previous single J' -selected PFI-PE measurements.^{12–15,21,22} Since the B^+ values for the (010) and (001) vibrationally excited states are not known, the B^+ value for the $\text{VCH}^+(\tilde{X}^2\Sigma^+; 000)$ ground state is used for simulations of these excited vibrational bands. As shown in the simulated state-to-state spectra of Figs. 2, 4(a), and 4(b), the maximum photoionization cross sections occur at the $|\Delta N^+| = 0$ transitions. The best simulated spectra reproduce the experimental IR-UV-PFI-PE spectra satisfactorily.

The simulation for the IR-VUV-PFI-PE spectrum of Fig. 2 yields the $\nu_{000}^+ = 54\,643 \pm 1\text{ cm}^{-1}$, which is in excellent agreement with the $\nu_{000}^+ = 54\,642.9 \pm 0.8\text{ cm}^{-1}$ determined by the analysis of the J' -selected and N^+ -resolved IR-UV-PFI-PE spectra of Figs. 3(a) and 3(b). The ν_{010}^+ and

ν_{001}^+ values determined by the spectral simulation are $55\,269 \pm 1$ and $55\,495 \pm 1\text{ cm}^{-1}$. Since $J'' = 1$ is the lowest rotational state of $\text{VCH}(\tilde{X}^3\Delta_1; 000)$, the IEs for the formation of $\text{VCH}^+(\tilde{X}^2\Sigma^+; 010)$ and 001 from $\text{VCH}(\tilde{X}^3\Delta_1; 000)$ are determined as $55\,268 \pm 1$ and $55\,494 \pm 1\text{ cm}^{-1}$, respectively. These values give the frequencies of 626 ± 1 and $852 \pm 1\text{ cm}^{-1}$ for the respective ν_2^+ and ν_3^+ vibrational modes of $\text{VCH}^+(\tilde{X}^2\Sigma^+)$, which are similar to the known vibrational frequencies⁵ of 578 and 855 cm^{-1} for the respective ν_2 and ν_3 vibrational modes of TiCH. The similar values observed for the ν_3^+ frequency for $\text{VCH}^+(\tilde{X}^2\Sigma^+)$ and the ν_3 ($= 838\text{ cm}^{-1}$) frequency for $\text{VCH}(\tilde{X}^3\Delta_1)$ are consistent with the finding that $D_0(\text{V}^+\text{-CH}) \approx D_0(\text{V-CH})$. The ν_2^+ frequency of $\text{VCH}^+(\tilde{X}^2\Sigma^+)$ is found to be significantly higher (by 62 cm^{-1}) than the ν_2 (564 cm^{-1}) frequency of $\text{VCH}(\tilde{X}^3\Delta_1)$. Since the excited ν_1^+ ($\text{V}^+\text{-H}$ stretching) vibrational band of $\text{VCH}^+(\tilde{X}^2\Sigma^+)$ was expected to be out of the energy range of the present experiment and thus was not measured, a direct comparison between the ν_1 frequency for $\text{VCH}(\tilde{X}^3\Delta_1)$ and ν_1^+ frequency for the ion cannot be made. On the basis of the higher $D_0(\text{V}^+\text{-CH})$ value compared to the $D_0(\text{V-CH})$ value observed here, we expect the ν_1^+ stretching frequency for $\text{VCH}^+(\tilde{X}^2\Sigma^+)$ to be higher than the ν_1 frequency for $\text{VCH}(\tilde{X}^3\Delta_1)$.

This work was supported by the NSF Grant No. CHE 0910488 and the U.S. Department of Energy (DOE), Basic Energy Sciences Contract No. DE-FG02-02ER15306.

- ¹D. Schroder and H. Schwarz, *Angew. Chem. Int. Ed. Engl.* **34**, 1973 (1995).
- ²J. F. Harrison, *Chem. Rev.* **100**, 679–716 (2000).
- ³M. Barnes, P. G. Hajigeorgiou, R. Kastai, A. J. Merer, and G. F. Metha, *J. Am. Chem. Soc.* **117**, 2096 (1995).
- ⁴S. M. Mattar and C. Kennedy, *Chem. Phys. Lett.* **238**, 230–235 (1995).
- ⁵M. Barnes, A. J. Merer, and G. F. Metha, *J. Mol. Spectrosc.* **181**, 168 (1997).
- ⁶W. H. Hocking, M. C. L. Gerry, and A. J. Merer, *Can. J. Phys.* **57**, 54 (1979).
- ⁷W. J. Balfour, A. J. Merer, H. Niki, B. Simard, and P. A. Hackett, *J. Chem. Phys.* **99**, 3288 (1993).
- ⁸O. Krechkivska and M. D. Morse, *J. Phys. Chem. A* **117**, 13284 (2013).
- ⁹E. W. Schlag, *ZEKE Spectroscopy* (Cambridge University Press, Cambridge, 1996).
- ¹⁰C. Y. Ng, *Ann. Rev. Phys. Chem.* **65**, 197–224 (2014).
- ¹¹J. Harrington and J. C. Weisshaar, *J. Chem. Phys.* **97**, 2809–2812 (1992).
- ¹²Y.-C. Chang, C.-S. Lam, B. Reed, K.-C. Lau, H. T. Liou, and C. Y. Ng, *J. Phys. Chem. A* **113**, 4242 (2009).
- ¹³H. Huang, Y.-C. Chang, Z. Luo, X. Shi, C.-S. Lam, K.-C. Lau, and C. Y. Ng, *J. Chem. Phys.* **138**, 094301 (2013).
- ¹⁴H. Huang, Z. Luo, Y.-C. Chang, K.-C. Lau, and C. Y. Ng, *J. Chem. Phys.* **138**, 174309 (2013).
- ¹⁵H. Huang, Z. Luo, Y.-C. Chang, K.-C. Lau, and C. Y. Ng, *Chin. J. Chem. Phys.* **26**, 669 (2013).
- ¹⁶Y.-C. Chang, Z. Zhang, Z. Luo, Y.-N. Song, Q. Z. Yin, and C. Y. Ng, “State-to-state photoionization dynamics of vanadium carbide by two-color laser photoionization and photoelectron methods” (unpublished).
- ¹⁷R. H. Page and S. Gudeman, *J. Opt. Soc. Am. B* **7**, 1761 (1990).
- ¹⁸K.-C. Lau and C. Y. Ng, *Acc. Chem. Res.* **39**, 823–829 (2006).
- ¹⁹N. Aristov and P. B. Armentrout, *J. Am. Chem. Soc.* **106**, 4065 (1984); **108**, 1806 (1986).
- ²⁰T. G. Dietz, M. A. Duncan, D. E. Powers, and R. E. Smalley, *J. Chem. Phys.* **74**, 6511 (1981).
- ²¹P. Wang, X. Xing, K.-C. Lau, H. K. Woo, and C. Y. Ng, *J. Chem. Phys.* **121**, 7049 (2004).
- ²²X. Xing, P. Wang, B. Reed, S. J. Baek, and C. Y. Ng, *J. Phys. Chem. A* **112**, 9277 (2008).